OPTICAL STUDIES OF NANOPHASE TITANIA

R. J. Gonzalez and R. Zallen

**in *Amorphous insulators and Semiconductors*,
edited by M. F. Thorpe and M. Mitkova
(Kluwer Academic Publishers, Dordrecht, 1997),
pp. 395-403.**

R.J. Gonzalez and R. Zallen, in Amorphous Insulators and Semiconductors edited by M.F. Thorpe and M. Mitkova (Kluwer Academic Publishers, Dordrecht, 1997). pp. 395-403: "Optical Studies of Nanophase Titania".

OPTICAL STUDIES OF NANOPHASE TITANIA

R. J. GONZALEZ and R. ZALLEN
Department of Physics, Virginia Tech
Blacksburg, VA 24061-0435 USA

1. Introduction

Titania, TiO_2, is a somewhat unlikely insulator to be included in this volume. To see this, we can compare it to SiO_2, the prototypical glass-forming insulating solid which features prominently in these proceedings.

Property	SiO_2	TiO_2
bonding	covalent	highly ionic
coordination	low (4,2)	high (6,3)
structural units	tetrahedra	octahedra
linkage	corner-sharing	edge-sharing
Zachariasen rules	OK	not OK
glass former	among the best	among the worst

Although it is a rotten glass-former, amorphous TiO_2 can, in fact, be prepared by sol-gel techniques. Its atomic-scale structure has been studied [1], and its optical properties (Raman and infrared) will appear briefly in the present article. So it is not the worst glass former mentioned in these proceedings; that honor probably belongs to KCl. The present article will deal mainly with nanophase titania, characterized by particle sizes under 100 nm in size.

The high ionicity of TiO_2, and its consequent high dielectric constant (roughly 50, depending on direction and crystal phase), makes it a candidate to replace silicon oxide and silicon nitride (two very important amorphous insulators) as the dielectric layer in the next generation of ultrathin thin-film capacitors. This is its most important high-tech application. Titania already has plenty of low-tech applications. It is the world's most important white pigment; well over 10^9 kg/year is produced for paint. Among its material properties are polymorphism (three crystal phases coexist indefinitely at ordinary conditions), high refractive index, transparency in the visible, and complete nontoxicity. Applications related to the last two include its use as an ultraviolet-absorbing optical filter and as a whitener in toothpaste.

M. F. Thorpe and M. I. Mitkova (eds.), Amorphous Insulators and Semiconductors, 395–403.

TiO_2 also is used as a catalyst support, since it can be prepared in the form of ultrafine nanometer-scale particles. One way of doing this is with sol-gel techniques. In this article, we describe some results recently obtained at Virginia Tech on optical studies of nanophase titania obtained by thermal and other treatments of sol-gel titania particles.

2. Sol-Gel Synthesis

The metal alkoxide used as the precursor is $Ti(OC_2H_5)_4$, called titanium tetraethoxide or tetraethylorthotitanate (TEOT). A simplified statement of the chemistry [2] is:

hydrolysis, $$Ti(OC_2H_5)_4 + 4H_2O \rightarrow Ti(OH)_4 + 4C_2H_5OH;$$

condensation, $$Ti(OH)_4 \rightarrow TiO_2 + 2H_2O.$$

An important variable is the water concentration relative to the alkoxide, given by the molar ratio $R=[H_2O]/[TEOT]$. Edelson and Glaeser [3] introduced a water soluble polymeric surfactant, hydroxypropylcellulose (HPC), into the sol-gel procedure in order to stabilize small particle sizes; the polymer adsorbs onto the forming particles and provides steric hindrance that impedes aggregation. In our work, we used variations on this technique (varying R, using HPC or omitting it, etc.); details are given elsewhere [4].

3. Infrared Reflectivity of Bulk and Nanophase Anatase TiO_2

Three crystal forms of titania are found in nature: rutile, anatase, and brookite. Rutile is the "true" stable phase at standard temperature and pressure (in the sense that graphite is the "true" stable phase of carbon at STP), and it is by far the most-studied and best-understood phase. Large single crystals of rutile have long been available, and the lattice dynamics of rutile TiO_2 in the lattice-fundamentals regime has been studied by polarization-dependent far-infrared reflectivity measurements [5]. This is not the case for anatase TiO_2. The polarization-dependent single-crystal far-infrared reflectivity of anatase has only recently been measured [6] by our group. The results are shown in Fig. 1.

The clean polarization-dependent reflectivity spectra of Fig. 1, along with the theoretical fits shown [5], determine the transverse-optical (TO) and longitudinal-optical (LO) zone-center infrared-active phonon frequencies for anatase. For E//c, $\overline{\nu}(TO)$ is 367 cm^{-1} and $\overline{\nu}(LO)$ is 755 cm^{-1}; for E⊥c, the two TO/LO pairs are

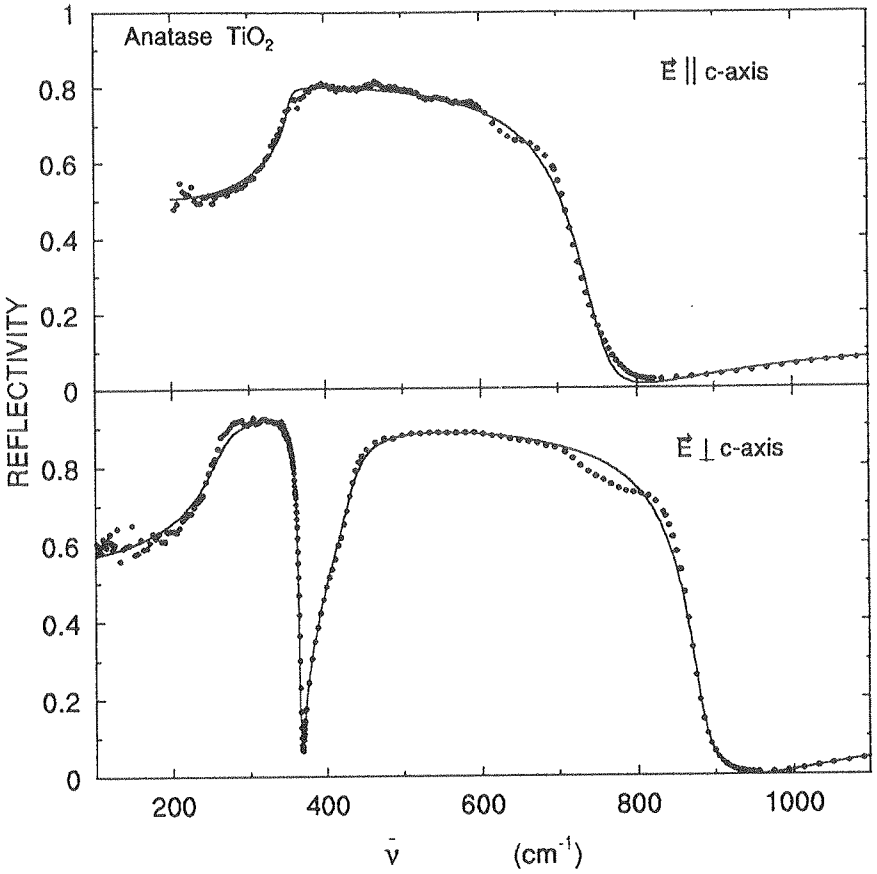

Figure 1. The polarization-dependent far-infrared reflectivity of single-crystal anatase. The curves are fits based on the factorized form of the dielectric function.

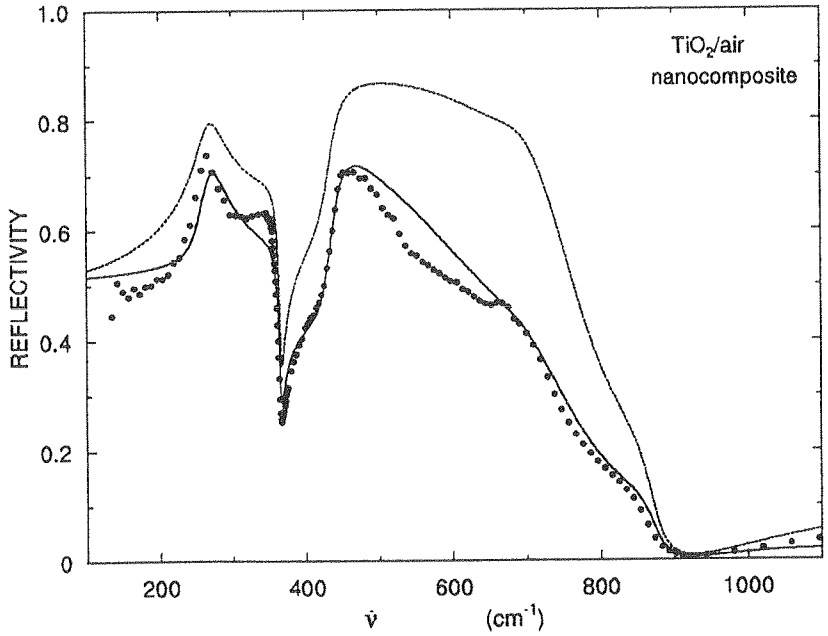

Figure 2. The infrared reflectivity of a pressed pellet prepared from sol-gel titania particles annealed at 600°C, analyzed with a combination of effective medium theory, bulk crystal data, and surface roughness. The dashed curve corresponds to the assumption of an abrupt air/pellet interface, the solid curve corresponds to the assumption of a graded surface layer of thickness 1.5 μm.

262/366 and 435/876 cm^{-1}. The very large TO-LO splittings demonstrate the high ionicity of anatase TiO_2.

In Fig. 2, we show the results of infrared reflectivity measurements on a dense pressed pellet of nanophase anatase. As discussed in the following section, we have studied annealing-induced phase transformations in sol-gel titania. Anatase dominates for anneal temperatures between 300 and 800°C. The pressed pellet of Fig. 2 was prepared from sol-gel particles and then annealed in pellet form at 600°C. X-ray diffraction linewidth measurements determined the average nanocrystallite size to be 50 nm. This spectrum was first analyzed using the crystal dielectric functions (determined from Fig. 1) and the Bruggeman effective medium theory [7]. The model assumes the pellet to be a composite of two fictitious isotropic materials, one having dielectric function $\varepsilon_{//}$ and the other having dielectric function $\varepsilon_{\perp}$. Effective medium theory was then used to estimate ε_{pellet} of the composite, assuming volume fractions of 1/3 (for $\varepsilon_{//}$) and 2/3 (for $\varepsilon_{\perp}$). The result is the dashed curve of Fig. 2 which, though containing the main qualitative features of the observed spectrum, is not quantitatively close for the vertical scale.

The dashed curve discussed above assumes the usual abrupt air/pellet interface. The solid curve shown in Fig. 2 incorporates the effect of surface roughness; a graded surface layer of 1.5 μm thickness was used here. Effective medium theory is again used to optically characterize the graded layer, but now the two components are taken to have dielectric functions ε_{pellet} (for nanocrystalline anatase) and 1.00 (for air). This method is rather successful.

4. Annealing-Induced Phase Transformations

Optical techniques are effective for studying the phase transformations that occur upon annealing sol-gel titania. Figure 3 presents a series of Raman-scattering spectra observed after anneals up to 1000°C. The Raman spectra were taken at room temperature, using the argon green line. Anneals were done in air for 40 minutes.

X-ray diffraction studies [1] have shown that the as-grown titania is amorphous, and this is revealed in the Raman spectra by the broad overlapping bands seen at the lower left of Fig. 3. Three spectra are shown for 250°C. These correspond to data taken with a Raman microprobe at different parts of the sample. The sharp, strong, anatase band at 141 cm^{-1} is already present at T_{anneal} = 250°C, indicating that some crystallization (into the anatase phase) has occurred although the material is still primarily amorphous. Conversion to anatase is complete by about 400°C. Anatase dominates for anneals to 700°C. Rutile appears alongside anatase at T_{anneal} = 800°C, and conversion to rutile is complete at 1000°C.

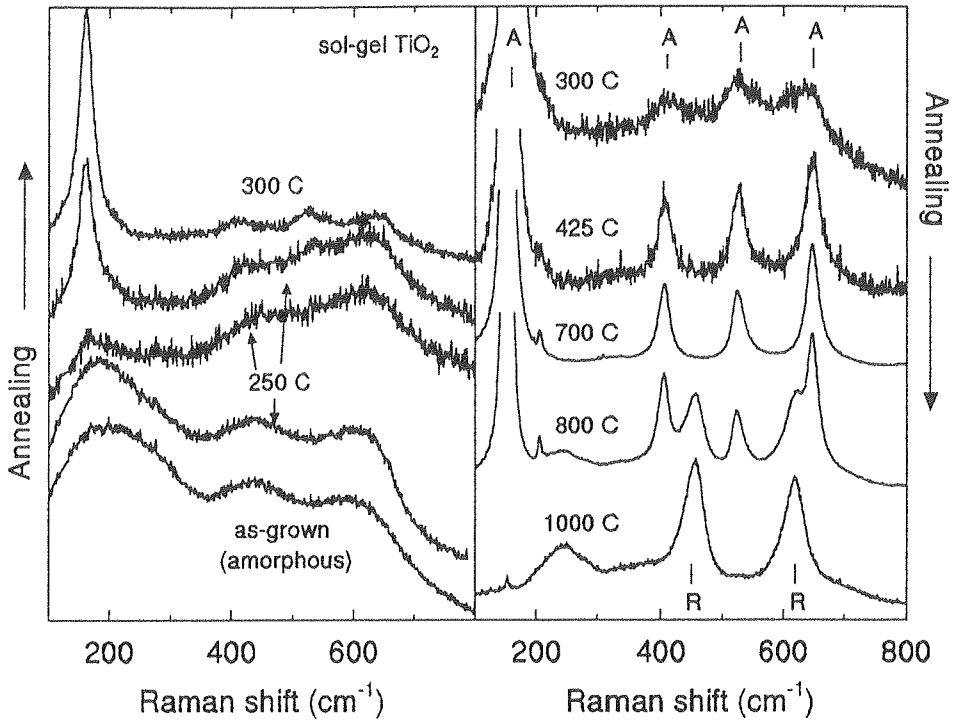

Figure 3. Room-temperature Raman spectra of ultrafine sol-gel titania particles, after annealing in air to different temperatures. The spectra clearly display the progression from amorphous TiO_2 to the anatase (A) and then the rutile (R) crystal forms.

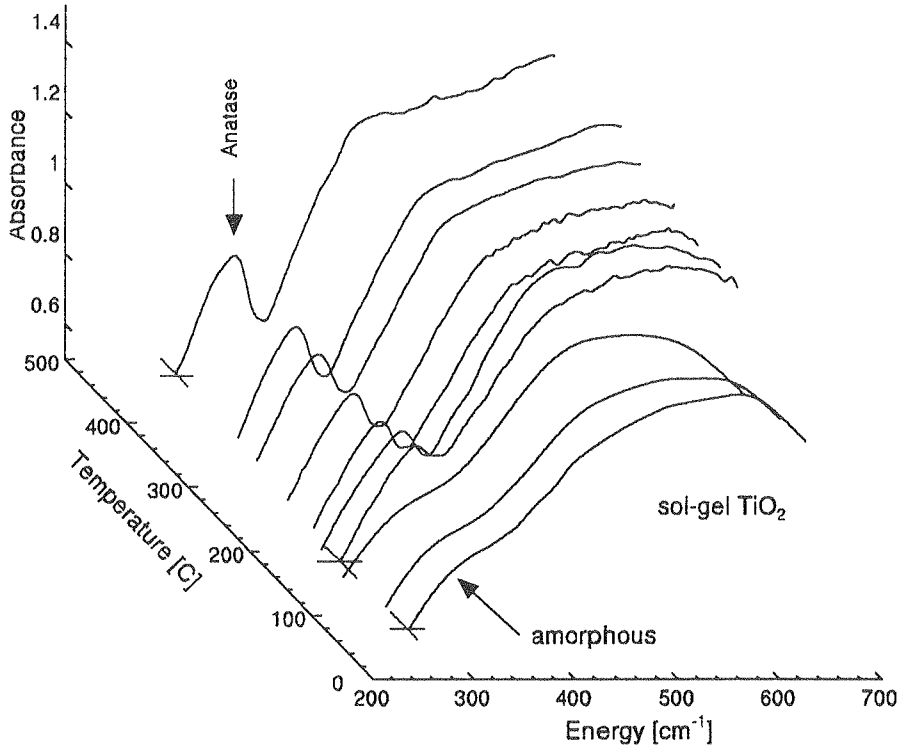

Figure 4. Infrared absorption spectra of sol-gel TiO_2 particles, diluted in KBr and pressed into pellets. These are in-situ temperature-dependent measurements.

Figure 4 displays infrared absorption measurements on the titania particles, taken during annealing. Unlike the Raman results, these are in-situ measurements taken while the sample was at elevated temperature. Powder samples were diluted in KBr (0.5% titania, by weight), pressed into pellets, and mounted in an optically accessible heater located within the evacuated sample space of a Bomem FTIR spectrometer. The heating rate was 1.25°C/min. A characteristic anatase band near 360 cm^{-1} clearly makes its appearance by 200°C, even though the material is still mainly amorphous (from x-ray and Raman) at this temperature.

5. Search for Finite-Size Effects in Anatase Raman Spectra

In semiconductors [8], AlO(OH) [9], and some other crystals, there is a well-documented finite-size effect observed for nanocrystalline samples; Raman bands broaden and shift with decreasing nanocrystal size L. The mechanism is as follows. For a nanocrystal of size L, the strict infinite-crystal k-space selection rule is replaced by a relaxed version characterized by a k-space uncertainty of about (1/L). Instead of k=0 only, a range of k-values from 0 to (1/L) are now Raman-allowed. Since the phonon dispersion curve $\nu(k)$ is not flat, the observed Raman band shifts and broadens. The smaller the L, the larger is the shift and broadening.

Because the anatase phase was the dominant form over a wide range of anneal temperatures (Fig. 3), and because the average nanocrystal size increases with annealing, we have looked for a finite-size effects in the Raman spectrum of nanocrystalline anatase. Crystallite sizes (L) were estimated from the linewidth of the (101) anatase peak observed in x-ray diffraction.

Figure 5 shows a comparison of the Raman spectrum of "bulk" anatase (micron-size crystals) with that of a nanocrystalline powder obtained by annealing sol-gel particles in air at 300°C. The strong and sharp bulk-anatase line at 141 cm^{-1} broadens and blue-shifts, while the 638 cm^{-1} band broadens and red-shifts. We have followed in detail the peak position and the linewidth (full width at half maximum) of the dominant 141 cm^{-1} Raman band, during the course of annealing.

Two different annealing atmospheres were used, air and argon, because it is known that stoichiometry changes can influence the Raman spectra of annealed TiO_2 particles [10]. Figure 6 shows a compilation of our results in the form of the correlation between the Raman-lineshape parameters (peak position ν and linewidth Γ of the 141 cm^{-1} anatase band) and the nanocrystal diameter L. Despite the scatter, it can be seen that the argon-annealed samples lie close to a single curve in each panel of Fig. 6. Similarly, all of the air-annealed samples lie close to a single curve in each panel of Fig. 6. But the argon

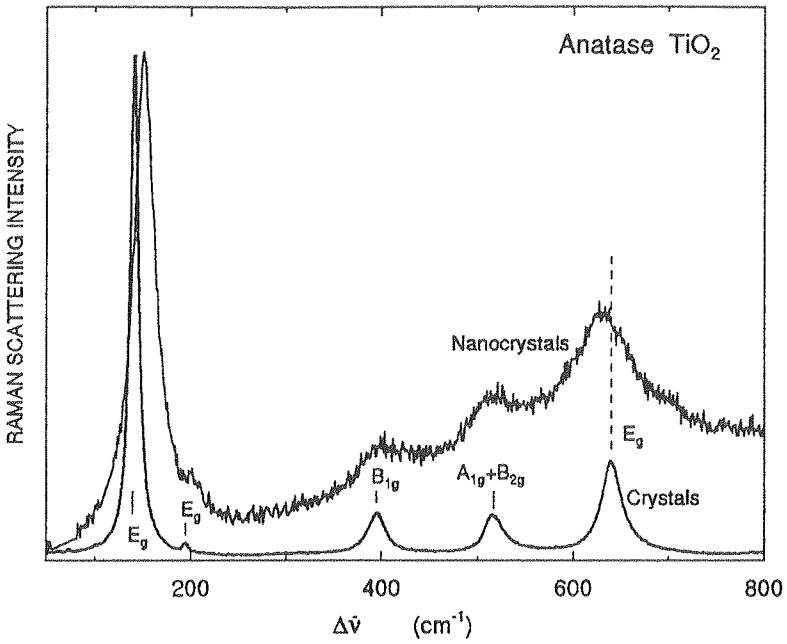

Figure 5. Comparison of the Raman spectrum of a nanocrystalline powder with that obtained from a powder of micron-size anatase crystals. The nanocrystalline sample was obtained by annealing sol-gel particles in air at 300°C.

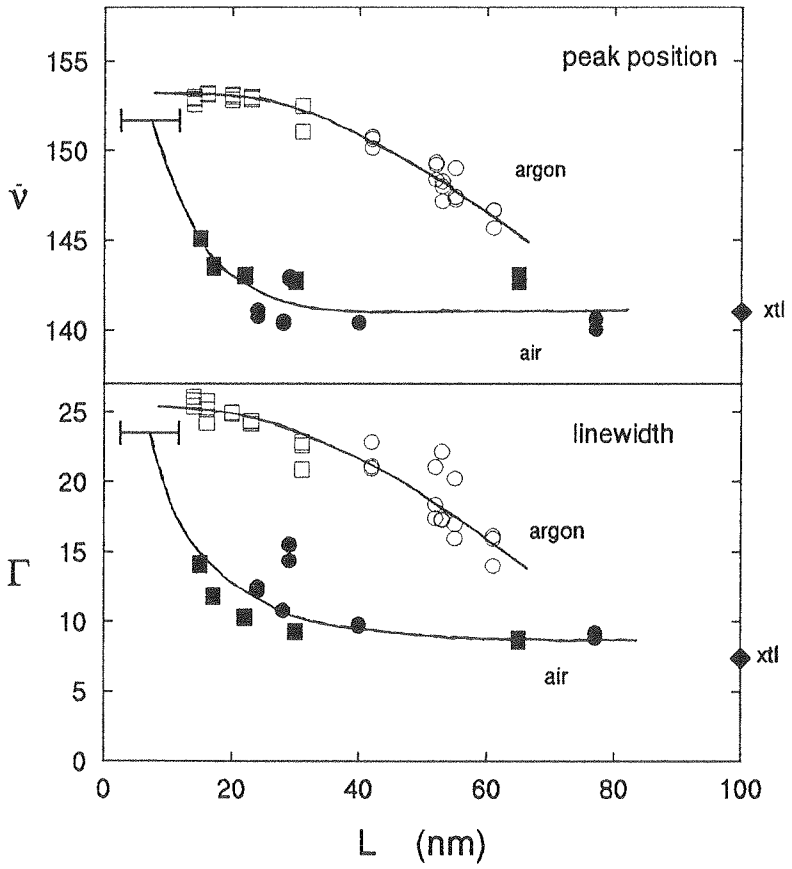

Figure 6. Raman lineshape versus nanocrystal size for the main anatase band of the annealed nanoparticles.

and air curves, for both $\nu(L)$ and $\Gamma(L)$, are distinctly different from each other. The argon curves make it only part way to the bulk-crystal values, while the air curves quickly approach the bulk values (becoming indistinguishable from them by L = 40 nm).

If L was the only physical quantity governing the changes in the Raman spectra, then each panel of Fig. 6 would contain a single curve. But this is not the case. The air/argon differences must be ascribed to the influence of stoichiometry [10].

For the air anneals, the initial rapid approach to the bulk-crystal values is then attributed to uptake of oxygen and the approach to stoichiometry of initially oxygen-deficient material. For the argon anneals, there is little effect because stoichiometry is little affected. From the Raman linewidth of 25 cm^{-1} for our small-L samples and the linewidth-versus-stoichiometry results of Parker and Siegel [10], it appears that the initial stoichiometry is $TiO_{1.98}$.

Since our results are interpretable on the basis of stoichiometry changes, no claim can be made here for the observation of finite-size effects. However, the following coincidence (?) is worth noting. Using the known dispersion curves of corresponding phonon modes in rutile, we have calculated the expected finite-size effects for the 141 and 638 cm^{-1} anatase bands. The calculated effects have the same signs (blue-shift for 141, red-shift for 638) and same relative sizes (large for 141, small for 638) as the observed effects. It therefore seems that phonon dispersion, the sign and size of the $\nu(k)$ curvature near k=0, also plays an important role in the sensitivity to stoichiometry of a Raman band.

6. Summary

A variety of optical and annealing investigations were performed on nanophase titania prepared by sol-gel techniques. The TO and LO frequencies of anatase were obtained from clean polarization-dependent infrared reflectivity measurements (Fig. 1) and, in combination with effective medium theory and the inclusion of surface roughness, were used to account for the infrared reflectivity of polycrystalline anatase (Fig. 2). Raman and infrared spectra were obtained for amorphous titania and were used to monitor amorphous-to-anatase and anatase-to-rutile annealing-induced phase transformations (Figs. 3 and 4). Extensive studies were done on the Raman spectra of anatase nanocrystals (Figs. 5 and 6). These have confirmed the importance of stoichiometry considerations, although interesting similarities to calculated finite-size effects indicate that phonon dispersion may also play a role in the sensitivity to stoichiometry.

7. Acknowledgments

We wish to thank the following individuals, each of whom has either collaborated with us on parts of this work or has helped us in other ways: A. Gaynor, R. M. Davis, H. Berger, R. J. Bodnar, and F. Harrison.

8. References

1. Wang, Q.J., Moss, S.C., Shalz, M.L., Glaeser, A.M., Zandbergen, H.W., and Zschack, P. (1992) in *Physics and Chemistry of Finite Systems: From Clusters to Crystals*, edited by P. Jena et. al., Kluwer Academic Publishers, Dordrecht.
2. Barringer, E.A. and Bowen, H.K. (1982) *J. Am. Ceram. Soc.* **65**, C-199; Barringer, E.A. and Bowen, H.K. (1985) *Langmuir* **1**, 414.
3. Edelson, L.H. and Glaeser, A.M. (1988) *J. Am. Ceram. Soc.* **71**, C-198.
4. Nagpal, V.J., Davis, R.M., and Riffle, S.J. (1994) *Colloids and Surfaces* **A 87**, 25; Gonzalez, R.J., Gaynor, A., Zallen, R., and Davis, R.M., to appear in *J. Mater. Res.*
5. Spitzer, W.G., Miller, R.C., Kleinman, D.A., and Howarth, L.E. (1962) *Phys. Rev.* **126**, 1710; Gervais, F. and Piriou, B. (1974) *J. Phys. C* 7, 2374.
6. Gonzalez, R.J., Zallen, R., and Berger, H. submitted to *Phys. Rev. B.*
7. Bruggeman, D.A.G. (1935) *Ann. Phys. (Leipzig)* **24**, 636; Aspnes, D.E. (1982) *Am. J. Phys.* **50**, 704.
8. Richter, H., Wang, Z.P., and Ley, L. (1981) *Sol. St. Commun.* **39**, 625; Nemanich, R.J., Solin, S.A., and Martin, R.M. (1981) *Phys. Rev. B* **23**, 6348; Tiong, K.K., Amirtharaj, P.M., Pollak, F.H., and Aspnes, D.E. (1984) *Appl. Phys. Lett.* **44**, 122; Holtz, M., Zallen, R., Brafman, O., and Matteson, S. (1988) *Phys. Rev. B* **37**, 4609; Zallen, R. (1992) *J. Non-Cryst. Solids* **141**, 227.
9. Doss, C.J. and Zallen, R. (1993) *Phys. Rev. B* **48**, 15626.
10. Parker, J.C. and Siegel, R.W. (1990) *J. Mater. Res.* **4**, 1246; Parker, J.C. and Siegel, R. W. (1990) *Appl. Phys. Lett.* **57**, 943.

Amorphous Insulators and Semiconductors

edited by

M. F. Thorpe
Department of Physics and Astronomy,
Michigan State University,
East Lansing, Michigan, U.S.A.

and

M. I. Mitkova
Central Laboratory of Electrochemical Power Sources,
Bulgarian Academy of Sciences,
Sofia, Bulgaria

Kluwer Academic Publishers

Dordrecht / Boston / London (1997)

Published in cooperation with NATO Scientific Affairs Division

REFERENCES

1. Q.J. Wang, S.C. Moss, M.L. Shalz, A.M. Glaeser, H.W. Zandbergen, and P. Zshack (1992) in *Physics and Chemistry of Finite Systems: From Clusters to Crystals*, *Vol. II*, edited by P. Jena *et al.*, Kluwer Academic Publishers, Dordrecht.
2. E.A. Barringer and H.K. Bowen (1982) *J. Am. Ceram. Soc.* **65**, C-199; E. A. Barringer and H.K. Bowen (1985) *Langmuir* **1**, 414.
3. L.H. Edelson and A.M. Glaeser (1988) J*. Am. Ceram. Soc.* **71**, C-198.
4. V.J. Nagpal, R.M. Davis, and S.J. Riffle (1994) *Colloids and Surfaces* **A 87**, 25; R.J. Gonzalez, A. Gaynor, R. Zallen, and R.M. Davis, to appear in *J. Mater. Res.*
5. W.G. Spitzer, R.C. Miller, D.A. Kleinman, and L.E. Howarth (1962) *Phys. Rev.* **126**, 1710; F. Gervais and B. Piriou (1974) *J. Phys. C* **7**, 2374.
6. R.J. Gonzalez, R. Zallen, and H. Berger, *Phys. Rev. B* **55**, 7014 (1997).
7. D.A.G. Bruggeman (1935) *Ann. Phys. (Leipzig)* **24**, 636; D.E. Aspnes (1982) *Am. J. Phys.* **50**, 704.
8. H. Richter, Z.P. Wang, and L. Ley (1981*) Sol. St. Commun.* **39**, 625; R.J. Nemanich, S.A. Solin, and R.M. Martin (1981) *Phys. Rev. B* **23**, 6348; K.K. Tiong, P.M. Amirtharaj, F.H. Pollak, and D.E. Aspnes (1984) *Appl. Phys. Lett.* **44**, 122; M. Holtz, R. Zallen, O. Brafman, and S. Matteson (1988) *Phys. Rev. B* **37**, 4609; R. Zallen (1992) *J. Non-Cryst. Solids* **141**, 227.
9. C.J. Doss and R. Zallen (1993) *Phys. Rev. B* **48**, 15626.
10. J.C. Parker and R.W. Siegel (1990) *J. Mater. Res.* **4**, 1246; J.C. Parker and R.W. Siegel (1990) *Appl. Phys. Lett.* **57**, 943.